

Large Volcanic Event on Io Inferred from Jovian Sodium Nebula Brightening

JEFFREY P. MORGENTHALER,¹ JULIE A. RATHBUN,¹ CARL A. SCHMIDT,² JEFFREY BAUMGARDNER,² AND
NICHOLAS M. SCHNEIDER³

¹*Planetary Science Institute
1700 East Fort Lowell, Suite 106
Tucson, AZ 85719-2395, USA*

²*Center for Space Physics
Boston University*

Boston, MA 02155, USA

³*University Of Colorado, Boulder
Boulder, CO 80309, USA*

(Received December 3, 2018; Revised January 10, 2019; Accepted January 10, 2019)

Submitted to ApJL

ABSTRACT

Using narrow-band images recorded on over 150 nights by the 35 cm coronagraph which comprises PSI’s Io Input/Output Facility (IoIO), we detected a 6-month long enhancement in the Jovian sodium nebula. The onset of the enhancement occurred in the mid December 2017 – early January 2018 timeframe. Sodium emission over the IoIO 0.4° field-of-view of was seen to increase through January 2018 and peak in early March 2018. By early June 2018, the surface brightness of the emission returned to the value seen 2017 April – June, making this the longest such event observed by this technique (Brown & Bouchez 1997; Yoneda et al. 2015) and comparable in length to that observed by the *Galileo* Dust Detector in 2000 (Krüger et al. 2003). A new IR hot-spot was found on Io near Susanoo/Mulungu paterae between January 2 and 12, however this hot-spot was neither bright nor long-lasting enough to have been independently identified as the source of a major sodium nebula enhancement. Furthermore, no other report of this event has been made despite a significant number of observations of the Jovian system by and in support of NASA’s *Juno* mission. This detection therefore places those observations in valuable context and highlights the importance of synoptic observations by facilities such as IoIO, which provide a global view of neutral material in the Jovian magnetosphere.

Keywords: planets and satellites: individual (Jupiter, Io) — instrumentation: miscellaneous

1. INTRODUCTION

Io’s volcanism was first hinted at by a fortuitous observation in the 3 – 5 μm region of the infrared (Witteborn et al. 1979), though it was not understood as such until after *Voyager 1* observations confirmed the presence of plumes (Morabito et al. 1979; Sinton 1980). This volcanism helped to place in context earlier fortuitous observations of Io’s ionosphere (Kliore et al. 1975), a sodium cloud near Io (Brown & Chaffee 1974), and ionized sulfur emission near Jupiter (Kupo et al. 1976): Io has an atmosphere which ultimately derives its source from volcanic activity and supplies Jupiter’s magnetosphere with a substantial amount of material ($\sim 1 \text{ ton s}^{-1}$, e.g., McGrath et al. 2004; Schneider & Bagenal 2007). As discussed in these references, material that is ionized forms the Io plasma torus (IPT), which encircles Jupiter near Io’s orbital radius. It is the bright line of singly ionized sulfur at [S II] 6731 Å which led to the initial detection of the IPT and has enabled it to be imaged by ground-based coronagraphs with apertures as small as 30 cm (Nozawa et al. 2004). Interaction between the IPT and Io’s atmosphere via processes such as sputtering,

charge exchanging and dissociative recombination, result in the energetic ejection of neutral material. Although a minor component of the material that is released, sodium has such bright doublet emission at 5890 Å and 5896 Å, that it has been imaged by ground-based coronagraphs with apertures as small as 10 cm (e.g., Mendillo et al. 1990, 2004; Yoneda et al. 2009, 2010, 2014, 2015).

Mendillo et al. (2004) used of order one wide-field (6°) sodium cloud image per year between 1990 and 1998 and a literature search of available Io infrared measurements to suggest there was a general correlation between the sodium nebula brightness and Io’s disk-averaged infrared brightness (their Figure 2). Long-lived volcanic hot spots, particularly Loki Patera and Tiermes Patera, were identified as the primary causes of this correlation (their Figure 1). Subsequent work by de Kleer, de Pater, & Yoneda (2016) used 3-years of higher cadence sodium cloud images (up to one per day) and much higher spatial resolution IR monitoring and failed to confirm this correlation. Rather, de Kleer, de Pater, & Yoneda (2016) suggested some, but not all, bright transient IR events traceable to individual volcanic eruptions may trigger sodium cloud brightening. Loki Patera and Tiermes Patera are lava lakes, which are not known to produce high eruptive plumes (e.g., Rathbun & Spencer 2006; de Pater et al. 2017). Rather, explosive events produced by volcanoes such as Pele, Tvashtar and Pillan (e.g., Jessup & Spencer 2012) would seem more likely to result in the ejection of material, though it is not clear if plume material from these eruptions can be ejected directly beyond Io’s atmosphere or if sublimation of the large ejecta blankets observed around these volcanoes is responsible for increase in ejection rates. Finally, Johnson et al. (1995) have suggested that SO₂ geysers may create “stealth plumes,” undetected by methods that monitor Io surface or near-surface properties, since they would not have strong infrared or dust signals. Regardless of the precise physical mechanism operating, Io’s volcanic nature is ultimately responsible for the release of gas into Jupiter’s magnetosphere. Therefore, for the purposes of this work, we will call such a release of gas a volcanic event.

Using a spectroscopic study that lasted an entire Jovian opposition, Brown & Bouchez (1997) showed that when there was a large increase in sodium emission in the inner Jovian magnetosphere, the IPT also became brighter and shifted to the east. The sodium peak brightness was seen before the IPT peak brightness. Brown & Bouchez (1997) attributed this behavior to an eruption of a volcanic plume on Io and the resulting radial and antisunward diffusion of material through the Jovian magnetosphere.

Yoneda et al. (2010) used the Nozawa et al. (2004) [S II] IPT observations and contemporaneously recorded small-aperture coronagraphic sodium nebula images to establish a correlation between IPT brightness and sodium nebula brightness in the same sense as that found by Brown & Bouchez (1997). Extreme ultraviolet (EUV) observations of the IPT have also shown evidence of correlation with indicators of volcanic ejection of material from Io (Krüger et al. 2003; Steffl et al. 2006; Yoneda et al. 2015; Kimura et al. 2018).

Motivated by the success of the small-aperture ground-based coronagraphic observations of the IPT and Jovian sodium nebula by Nozawa et al. (2004), Mendillo et al. (2004), and Yoneda et al. (2009, 2010, 2014, 2015) and the numerous open scientific questions in inner Jovian magnetospheric studies, we created the Io Input/Output facility (IoIO). Described in more detail in §2, IoIO is comparable in aperture size to the coronagraphs used by Nozawa et al. (2004) so that detection of the IPT in [S II] is possible. This makes the IoIO aperture area ~ 10 -times that of the wide-field sodium nebula studies of Mendillo et al. (2004) and Yoneda et al., with a comparable reduction in field-of-view. The larger aperture, yet still relatively large field-of-view (0.4°) simultaneously enables IoIO to study the detailed three-dimensional structure of the sodium nebula near Io and Jupiter (Figure 1 and on-line animation) and, like Yoneda et al., measure the average surface brightness of the Jovian sodium nebula with a nightly cadence. As detailed in §2 – §5, our reduction techniques are sufficient to demonstrate the detection of a large and long-term enhancement in the sodium nebula, however, removal of the effects of passing clouds is not yet as sophisticated as those of Yoneda et al.. As a result, the scatter our data is greater and the sensitivity to small enhancements is less. This will be addressed in subsequent iterations of our reduction pipeline. In §4 – §5 and Figure 2, we show that IoIO detected a substantial increase in the amount of sodium within ~ 50 Jovian radii (R_j) of Jupiter starting in the mid December 2017 – early January 2018 timeframe. In §6, we suggest this was caused by a volcanic event on Io.

2. OBSERVATIONS

The Io Input/Output facility (IoIO) consists of a 35 cm Celestron telescope feeding a custom-built coronagraph, a boresight-mounted 80 mm guide telescope and an Astro-Physics 1100 GTO German equatorial mount. IoIO is located at the San Pedro Valley Observatory, a hosting site situated in a dark location 100 km east of Tucson, Arizona, USA. The coronagraph imaging system is telecentric: A Kodak Wratten ND3 gelatin neutral density filter cut ~ 1.5 mm

Table 1. Filter Properties^a

Filter	CWL (Å)	FWHM (Å)
R	6349	1066
[S II] on-band	6731	10
Na on-band	5893	12
[S II] off-band	6640	40
Na off-band	6000	50

^aMeasured in a collimated, normal-incidence beam at 20° C

wide is placed at the focal plain of the Celestron telescope so that Jupiter is attenuated rather than occulted, allowing for astrometric and photometric calibrations. The diverging light from the f/11 beam then passes through one of the five filters listed in Table 1, which are standard bandpasses for this work. The filters are hard metal oxide coated to maximize durability and minimize central wavelength (CWL) temperature drift ($<0.1 \text{ \AA C}^{-1}$). The narrow-band Fabry-Pérot type filters, fabricated by Custom Scientific, have a very flat-topped profile with $>90\%$ peak efficiency. The sodium on-band filter was constructed such that both the Na D lines are transmitted with $<1\%$ change in efficiency over the entire FOV and nighttime temperature range expected at our hosting site. After the filters, the light passes through a field lens which focuses the telescope pupil onto the pupil of a Nikon Nikkor 60 mm F/2.8 camera lens. Finally, the light is collected by a Starlight Xpress SX694 medium format CCD camera. The effective focal length of IoIO is 1200 mm, the FOV for sodium nebula observations is 0.4° or $64 R_j - 84 R_j$, depending on Jupiter’s geocentric distance and pixels are $0.78''$ per side.

Sodium observations are recorded in on-band/off-band pairs for five minutes and one minute, respectively, every ~ 30 minutes. On- and off-band images of the Io plasma torus in [S II] 6731 Å are recorded on a 6-minute cadence in the intervals between the Na observations and will be reported in another work.

3. DATA REDUCTION

Because the sodium nebula is a field-filling source for our FOV, we take some care in reducing the data. This starts with the bias and dark subtraction of our on- and off-band images. The IPT is a much smaller target than the sodium nebula, so as a cost-savings measure, we used 32 mm diameter [S II] on- and off-band filters compared to the 50 mm Na filters. The small [S II] filter diameters enabled us to use pixels on the edges of the [S II] FOVs, to construct a near continuous record of the combined effects of bias and dark current through each night. These values were interpolated in time and subtracted from the Na on- and off-band images.

Sky flats show that white light vignetting is $\sim 10\%$ starting beyond the region we use for our analyses, so we ignore the effect. Similarly, we ignore small-scale variation in biases, flats, and darks since our primary results are derived by averaging over large areas of pixels.

After bias and dark subtraction, we subtract the off-band image recorded closest in time from each on-band image. A factor, OFFSCALE, is multiplied by each off-band image. OFFSCALE is the product of the flux in the central 10×10 pixel ($7.8'' \times 7.8''$) areas of Jupiter in the on- and off-band images times. An additional factor of 0.80 is applied to remove over-subtraction consistently seen in the images. OFFSCALE typically varies by $\sim 20\%$ each night and there was a systematic drop of 20% during April attributable to improvements we were making in the guiding system: because on-band images have longer exposure times than off-band, improved guiding reduced smearing of Jupiter preferentially in the on-band images, hence raising OFFSCALE. We show in §5 that the systematic change in OFFSCALE has no effect on our results.

We derive a factor, ADU2R, to convert pixel values to the surface brightness unit of rayleighs (R) where $1 \text{ R} = \frac{10^6}{4\pi} \text{ photons s}^{-1} \text{ cm}^{-1} \text{ sr}^{-1}$:

$$\text{ADU2R} = \frac{on_jup * ND}{MR} \quad (1)$$

Here, *on_jup* is the average pixel value of the 10×10 pixel box centered on Jupiter in the on-band images. This area represents pixels within $\sim 0.2 R_j$ of the center of Jupiter. ND is the attenuation factor provided by our neutral density filter. R-band measurements of GSC5017:78 on 2018-03-20UT show $ND = 730 \pm 70$. MR is the surface brightness of Jupiter over our 12 Å-wide bandpass on-band filter. To account for the deep sodium Fraunhofer absorption lines, this

is calculated using Jovian albedos from [Woodman et al. \(1979\)](#) and [Karkoschka \(1998\)](#), see also PDS: ESO-J/S/N/U-SPECTROPHOTOMETER-4-V2.0) and the [Kurucz \(2005\)](#) solar flux atlas. MR varied from 52.6 MR to 54 MR over the IoIO observations.

Figure 1 shows two of the over 700 images of the sodium nebula recorded by IoIO and processed as described above. Data were recorded on over 150 nights between IoIO commissioning in March 2017 and the end of the Jovian opposition in July 2018. Subsequent work will address the “banana,” “jet,” and “stream” features described in the caption of Figure 1. For our current work, we concentrate on the diffuse emission in the images, which can be studied using the surface brightness in various apertures centered on Jupiter. In §4 and Figure 2, we present the time evolution of these surface brightness values to show that there was a large modulation in the emission detected by IoIO during the 2018 Jovian opposition. In §5, we demonstrate that this emission was from the Jovian sodium nebula.

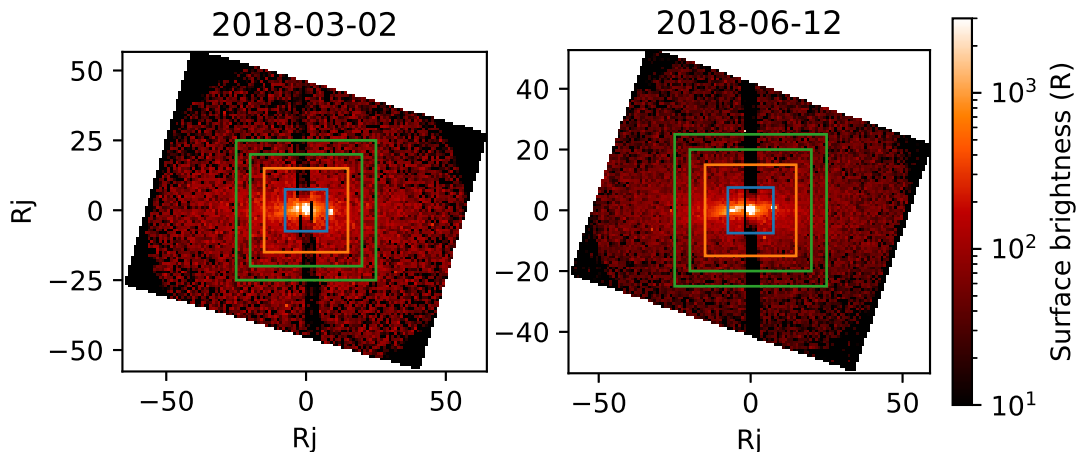


Figure 1. Two images of the inner 0.4° ($\sim 50 R_j$) of the Jovian sodium nebula recorded by IoIO. Left: image recorded 2018-02-27 08:26:11 UT, during the period when the extended Jovian sodium nebula was bright. Right: image recorded 2018-06-12 04:40:37 UT, during a period when the nebula was at baseline value. The images have been down-sampled by a factor of four [five for arXiv e-print] and then rebinned by another factor of four [five for arXiv e-print]. The boxes indicate the apertures used to construct Figure 2 (left). The innermost aperture (blue) is a square area $15 R_j$ on a side containing points approximately within approximately $7.5 R_j$ from Jupiter (blue triangles in Figure 2, left). The next concentric aperture (orange) is a square aperture $30 R_j$ on a side containing points $< 15 R_j$ from Jupiter (orange squares in Figure 2, left). The square annular area, between the outermost two (green) rectangles was used to calculate the surface brightnesses shown as the green Xs in Figure 2 (left and right). This corresponds to points $20 R_j < r < 25 R_j$, which is comparable to the $25 R_j$ aperture used by [Yoneda et al. \(2009\)](#). An animation, lasting 1.5 min, of the dataset is found in the online Journal and shows the 3-D structure of the “banana,” “jet” and “stream” features discovered by [Schneider et al. \(1991\)](#) and modeled in detail by [Wilson et al. \(2002\)](#). Individual frames of the animation have been processed with the histogram equalization method to enhance contrast of low surface brightness features. Frames with high background light (average surface brightness $> 250 R$) have been removed, as have frames where the image of Jupiter moved more than 5 pixels between the on-band and off-band images. The later effect does not materially affect our aperture surface brightness values, but it does detract cosmetically from the animation. In the animation, values above 8 kR have been set to zero and Jupiter has been scaled up by a factor of 100. Long-term, an on-going archive of all raw and reduced images collected by IoIO will be kept at NASA’s Planetary Data System (PDS).

4. RESULTS

Figure 2 shows that there was a significant and long-lasting enhancement in emission detected by IoIO during the 2018 Jovian opposition. The left panel of the Figure shows via large colored triangles, squares and Xs, the nightly medians of the average surface brightnesses within the three regions indicated by colored squares in Figure 1. All of the surface brightness measurements for one of the apertures are shown as small black dots. The right panel of Figure 2 shows an 11-day moving median (blue histogram) which smooths the effects of variable weather. As discussed in more detail in §5, the enhancement bears the mark of modulation in brightness of a centrally peaked source because the more centrally concentrated apertures have larger modulations as a function of time. The extrapolation of the $20 R_j < r < 25 R_j$ aperture, shown in Figure 2 (right, orange line), suggests that the enhancement started no later than

early January 2018. The scatter in the data suggests the enhancement could have begun as early as mid-December 2017. The emission peaked in brightness in March and remained bright until 2018 June, making this 1.8 times longer than the events observed by [Brown & Bouchez \(1997\)](#) and [Yoneda et al. \(2015\)](#) and comparable in length to that observed by the *Galileo* Dust Detector in 2000 ([Krüger et al. 2003](#)). The intensity of the enhancement is discussed in more detail in §5.

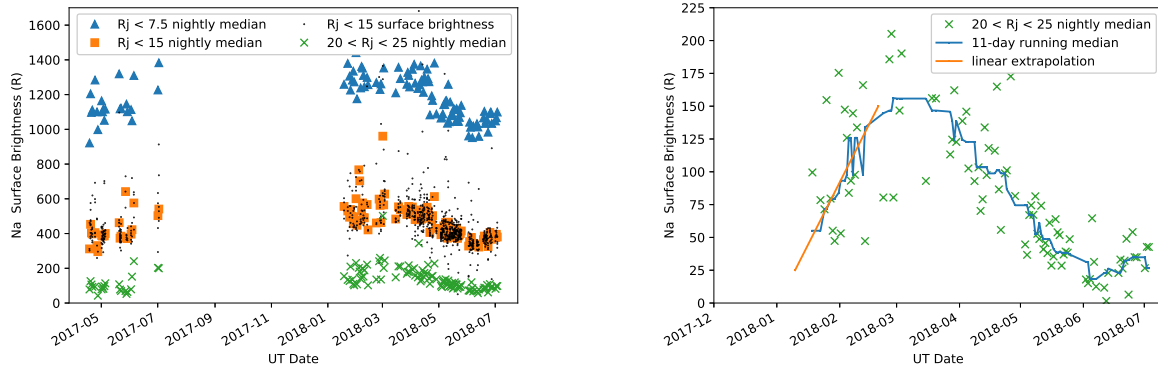


Figure 2. Left: Time history of the emission measured by IoIO for the apertures indicated in Figure 1. Section 5 provides the evidence that the long-term trend seen in these curves is long-term modulation in the Jovian sodium nebula surface brightness. Right: Time history of nightly medians from the $20 R_j < r < 25 R_j$ aperture with estimated mesospheric sodium emission subtracted (§5). An 11-day running median (blue histogram) is extended by a simple linear extrapolation (orange line) to indicate early January 2018 is the latest time the enhancement could have started. The code `read_ap.py` in [Morgenthaler \(2019\)](#) reads the aperture sum data file in [Morgenthaler et al. \(2019\)](#) to create both panels in the Figure.

5. DISCUSSION

As discussed in §2–§3, IoIO does not see to the edge of the Jovian sodium nebula. Furthermore, to maximize observing time on the plasma torus, sodium sky background observations away from Jupiter were not systematically recorded. Thus, we must take some care in our analyses to ensure we are detecting modulation in the Jovian sodium nebula and not some other source.

The first factor we consider which could possibly contribute to the long-term modulation seen in Figure 2 is improper subtraction of the continuum light recorded in our on-band images. This is particularly concerning given the systematic change in OFFSCALE noted in §3. We rule out this concern in several ways. First, the change in OFFSCALE occurred more abruptly in April compared to the decline seen in Figure 2. Second, we reversed the sense of the long-term change in OFFSCALE and re-processed images in March and June and found that the March aperture surface brightness values were still higher than the June. Perhaps most convincingly, we create plots like Figure 2 using our on-band and off-band images separately. These plots show more scatter than Figure 2, but the on-band plot already shows the trend seen in Figure 2. The off-band plot shows no long-term trend. These observations confirm that our background subtraction is reasonable and that the modulation seen in Figure 2 comes from line emission and not continuum emission in the on-band filter bandpass.

Next we consider the response of IoIO to the primary source of sodium emission other than the Jovian sodium nebula: the Earth’s mesospheric sodium layer. This layer is formed from the ablation of meteors. Its thickness has seasonal dependence in the same sense as the modulation seen in Figure 2 (e.g., [Dunker et al. 2015](#), their Figure 4), which is why it is of concern for our analyses. Mesospheric sodium also has a diurnal variation because it is excited by photochemical processes local to the layer (e.g., [Kirchhoff et al. 1979](#)). In contrast to this, the Jovian sodium nebula has negligible nightly modulation over the $\sim 3.5 \times 10^6$ km region covered by the IoIO FOV. Thus, by considering our data on a night-by-night basis, we can probe the response of IoIO to a uniform field-filling source without interference from the nebula. The black dots in Figure 2 (left) show the extent of the nightly modulations for the $r < 15 R_j$ aperture fall within the 40 R – 200 R range seen at other locations. Larger excursions, such as the last two nights in the 2017 observing season, recorded as the monsoon season started, are due to passing clouds. Nightly variations in emission

in all the apertures are highly correlated with correlation coefficients tending to one, as expected for variation in a uniform, field filling source. Thus, we simultaneously confirm with the IoIO data themselves the design criterion that IoIO’s detection efficiency is flat as a function of position (§2) and that seasonal modulation of a field-filling source would result in equal responses in all the apertures. We show in the next paragraph, this is not what is seen in Figure 2 (left).

To demonstrate that IoIO detected modulation in the brightness of the Jovian sodium nebula, we point out that the curve for each aperture in Figure 2 (left) has a unique shape. Relative to their respective baselines, the more centrally concentrated apertures have larger absolute amplitudes. This is the signature of modulation in the brightness of a centrally peaked source. The baseline values for our inner ($r < 7.5 R_j$), middle ($r < 15 R_j$), and outer ($20 R_j < r < 25 R_j$) apertures are $1030 \pm 30 R$, $370 \pm 25 R$, and $80 \pm 15 R$, respectively. The peak amplitudes of the middle and inner apertures are factors of ~ 1.5 and ~ 2.2 higher than the outer aperture, respectively. After removal of their respective baselines and scaling, the curves from the three apertures are in good agreement. Were we seeing seasonal modulation in the telluric sodium layer, the amplitudes would all have the same values in the same way that the nightly modulations do. This is our most convincing evidence that we are detecting modulation in the Jovian sodium nebula.

Although we have ruled out mesospheric emission as the cause of the long-term modulation seen in Figure 2 (left), we cannot rule out its contribution as a relatively stable background. In fact, we expect it. As discussed above, we did not record systematic sky background measurements, so this is not something that we can estimate independently. Instead, we compare the measured surface brightness in our outer aperture during the nebula’s quiescent state to the surface brightness of inner aperture used by Yoneda et al. (2009) during similarly quiet conditions. Both these apertures correspond to $r \sim 25 R_j$. As quoted above, the baseline in our outer aperture is $80 \pm 15 R$. The mesosphere-subtracted value quoted by Yoneda et al. (2009) is $20 R - 30 R$. This suggests that $50 R - 60 R$ of our emission is mesospheric, which is comparable to baseline values measured by this team at other locations. Subtracting this from our $r \sim 25 R_j$ aperture results in Figure 2 (right), which shows that the peak amplitude of the modulation observed in the Jovian sodium nebula at $r \sim 25 R_j$ is $155 \pm 25 R$ or a factor of ~ 2 larger than the $70 - 80 R$ peak in the event measured by Yoneda et al. (2009). The peak amplitude in the 2015 January to 2015 April enhancement reported by Yoneda et al. (2015) was a factor of ~ 1.5 larger than the Yoneda et al. (2009) enhancement. Thus, the 2018 enhancement detected by IoIO was a factor of ~ 1.3 brighter than the 2015 January to 2015 April enhancement reported by Yoneda et al. (2015).

6. CONCLUSION

We have detected a large and long-lasting enhancement in the Jovian sodium nebula. The extrapolation of the data shown in Figure 2 (right) suggests that the enhancement started no later than early January 2018. The scatter in the data suggests the enhancement could have begun as early as mid-December 2017. The calculations detailed in §5 suggests the event was $\sim 30\%$ brighter than the primary enhancement reported by Yoneda et al. (2015). The nebula remained bright until 2018 June, making this 1.8 times longer than the events observed by Brown & Bouchez (1997) and Yoneda et al. (2015) and comparable in length to that observed by the *Galileo* Dust Detector in 2000 (Krüger et al. 2003).

Infrared observations recorded at NASA’s IRTF by our team and at the W. M. Keck Observatory by K. de Kleer & I. de Pater as a continuation of the monitoring program discussed in de Kleer & de Pater (2016) achieved full longitudinal coverage of Io, but detected no IR-bright eruptions that lasted for over a month in the December 2017 to January 2018 timeframe. A new eruption near Susanoo/Mulungu paterae ($20^\circ N$ $218^\circ W$) was observed to begin sometime between January 2 and 12 (personal communication, de Kleer & de Pater, Dec. 2018). This event was $20 GW \mu m^{-1} sr^{-1}$ at brightest detected Lp ($3.78 \mu m$) and would therefore be classified as a faint eruption in the taxonomic scheme of de Kleer & de Pater (2016). The proximity in time between this eruption and the onset of the sodium nebula enhancement is suggestive but not conclusive evidence of a relationship. A more convincing case was made by de Kleer & de Pater (2016) that the two sodium nebula enhancements seen by Yoneda et al. (2015) were associated with two eruptions in the “mini-outburst” class at Kurdalagon Patera, as both eruptions were contemporaneous with the onset of the nebula enhancements. However, as noted by de Kleer, de Pater, & Yoneda (2016), during the three-year study of de Kleer & de Pater (2016), not all of the detected sodium nebula enhancements had identifiable IR counterparts. Along the same lines, the two Kurdalagon Patera outbursts were a factor of ~ 3 brighter than the eruption near Susanoo/Mulungu paterae, yet the two enhancements found by Yoneda et al. (2015) were not

of equivalent size nor were they larger than the enhancement reported here, as one would expect if IR brightness was correlated with the amount of gas released. The picture that emerges is that IR activity on Io is simply not predictive of sodium nebula enhancement. This observation is strengthened by the fact that all of the associations between IR eruptions and sodium nebula enhancements have been made *a posteriori*. This highlights the importance of synoptic observations of the Jovian sodium nebula for monitoring the supply of material to Jupiter’s magnetosphere – material that drives a host of magnetospheric phenomena.

With our detection of such a long-lasting event during the first half of the 2018 Jovian opposition, other observations may be placed in context. This is particularly important for observations conducted by *Juno*, large-aperture observatories, and *HST*, which themselves do not have synoptic coverage comparable to IoIO and were therefore not able to independently detect this event. For instance, our team regularly conducts observations of the IPT with the ARC 3.5 m telescope at Apache Point Observatory (Schmidt et al. 2018). In May 2018, these were seen to be the brightest yet recorded by this facility. Preliminary reduction of our IoIO [S II] images also shows evidence that the overall brightness of the IPT follows a similar envelope to that observed by Brown & Bouchez (1997) during the volcanic event they saw (§1). EUV observations of the IPT by *Hisaki* over this time period should be brighter than normal and show chemical and periodicity changes similar to those seen by Steffl et al. (2008) and Kimura et al. (2018) after volcanic events. We predict the neutral oxygen cloud around Jupiter, detectable with the *Hisaki* satellite (Koga et al. 2018a,b), will show higher values than found previously. Finally, higher than average auroral activity on Jupiter should be detected by *in situ* measurements from the *JUNO/JADE* instrument; in the UV by *Juno/UVS*, *Hisaki*, and *HST*; in the infrared by *Juno/JIRAM* and ground-based infrared telescopes; and in the radio by *Juno/WAVES* and ground-based radio telescopes such as the Nançay Decametric Array (e.g., McComas et al. 2017; Gladstone et al. 2017; Kimura et al. 2015; Kita et al. 2016; Kurth et al. 2017; Radioti et al. 2013; Marques et al. 2017).

Although we cannot provide independent measurement of the geological and atmospheric processes responsible for the production and release of gas detected from Io, we can use the shape of the 11-day running median in Figure 2 (right) to provide an estimate of the time evolution of the gas release, which, upon further study, may provide clues to its origin. Electron impact ionization is the primary loss mechanism of sodium within the IoIO FOV and is of order 10 – 20 days (e.g., Wilson et al. 2002, their Figure 3), which is short compared to the ~180 day enhancement in the nebula. Thus, the shape of the 11-day running median is primarily determined by the physical processes responsible for gas release from Io.

We thank Scott Tucker of Starizona for his excellent mechanical design and construction of the IoIO coronagraph and Vishnu Ready for helping to make that contact. We also acknowledge Dean Salman, manager of the San Pedro Valley Observatory, hosting site of IoIO, whose expertise at small-aperture astronomy was a major contributing factor to our ability to record scientifically useful images two weeks after the receipt of the last major and longest lead time parts (the filters). This work is supported by NSF grant AST 1616928 to the Planetary Science Institute.

Software: AstroPy (Astropy Collaboration et al. 2013), Astroquery (Ginsburg et al. 2013), ccdproc (Craig et al. 2015), Pythonaliasesandshortcuts (Morgenthaler & Morgenthaler 2019), DataThiefIII (Tummers 2006), IDL (Harris Geospatial Solutions 2018), IoIO control, reduction, and analysis software (Morgenthaler 2019), matplotlib (Hunter 2007), NumPy (Oliphant 2006), scikit-image (van der Walt et al. 2014)

REFERENCES

- Astropy Collaboration, Robitaille, T. P., Tollerud, E. J., et al. 2013, *Astron. Astrophys.*, 558, A33, doi: [10.1051/0004-6361/201322068](https://doi.org/10.1051/0004-6361/201322068)
- Brown, M. E., & Bouchez, A. H. 1997, *Sci*, 278, 268, doi: [10.1126/science.278.5336.268](https://doi.org/10.1126/science.278.5336.268)
- Brown, R. A., & Chaffee, Jr., F. H. 1974, *Astrophys. J., Lett.*, 187, L125, doi: [10.1086/181413](https://doi.org/10.1086/181413)
- Craig, M. W., Crawford, S. M., Deil, C., et al. 2015, ccdproc: CCD data reduction software, *Astrophysics Source Code Library*. <http://ascl.net/1510.007>
- de Kleer, K., & de Pater, I. 2016, *Icarus*, 280, 378, doi: [10.1016/j.icarus.2016.06.019](https://doi.org/10.1016/j.icarus.2016.06.019)
- de Kleer, K., de Pater, I., & Yoneda, M. 2016, AGU Fall Meeting Abstracts, P21E
- de Pater, I., de Kleer, K., Davies, A. G., & Ádámkóvics, M. 2017, *Icarus*, 297, 265, doi: [10.1016/j.icarus.2017.03.016](https://doi.org/10.1016/j.icarus.2017.03.016)
- Dunker, T., Hoppe, U.-P., Feng, W., Plane, J. M. C., & Marsh, D. R. 2015, *Journal of Atmospheric and Solar-Terrestrial Physics*, 127, 111, doi: [10.1016/j.jastp.2015.01.003](https://doi.org/10.1016/j.jastp.2015.01.003)

- Ginsburg, A., Robitaille, T., Parikh, M., et al. 2013, *Astroquery* v0.1, figshare, doi: [10.6084/m9.figshare.805208.v2](https://doi.org/10.6084/m9.figshare.805208.v2).
https://figshare.com/articles/Astroquery_v0.1/805208/2
- Gladstone, G. R., Persyn, S. C., Eterno, J. S., et al. 2017, *Space Science Reviews*, 213, 447, doi: [10.1007/s11214-014-0040-z](https://doi.org/10.1007/s11214-014-0040-z)
- Harris Geospatial Solutions. 2018, The Interactive Data Language. <https://www.harrisgeospatial.com>
- Hunter, J. D. 2007, *Computing In Science & Engineering*, 9, 90, doi: [10.1109/MCSE.2007.55](https://doi.org/10.1109/MCSE.2007.55)
- Jessup, K. L., & Spencer, J. R. 2012, *Icarus*, 218, 378, doi: [10.1016/j.icarus.2011.11.013](https://doi.org/10.1016/j.icarus.2011.11.013)
- Johnson, T. V., Matson, D. L., Blaney, D. L., Veeder, G. J., & Davies, A. 1995, *Geophys. Res. Lett.*, 22, 3293, doi: [10.1029/95GL03084](https://doi.org/10.1029/95GL03084)
- Karkoschka, E. 1998, *Icarus*, 133, 134, doi: [10.1006/icar.1998.5913](https://doi.org/10.1006/icar.1998.5913)
- Kimura, T., Badman, S. V., Tao, C., et al. 2015, *Geophys. Res. Lett.*, 42, 1662, doi: [10.1002/2015GL063272](https://doi.org/10.1002/2015GL063272)
- Kimura, T., Hiraki, Y., Tao, C., et al. 2018, *J. Geophys. Res.*, 123, 1885, doi: [10.1002/2017JA025029](https://doi.org/10.1002/2017JA025029)
- Kirchhoff, V. W. J. H., Clemesha, B. R., & Simonich, D. M. 1979, *J. Geophys. Res.*, 84, 1323, doi: [10.1029/JA084iA04p01323](https://doi.org/10.1029/JA084iA04p01323)
- Kita, H., Kimura, T., Tao, C., et al. 2016, *Geophys. Res. Lett.*, 43, 6790, doi: [10.1002/2016GL069481](https://doi.org/10.1002/2016GL069481)
- Kliore, A. J., Fjeldbo, G., Seidel, B. L., et al. 1975, *Icarus*, 24, 407, doi: [10.1016/0019-1035\(75\)90057-3](https://doi.org/10.1016/0019-1035(75)90057-3)
- Koga, R., Tsuchiya, F., Kagitani, M., et al. 2018a, *Icarus*, 299, 300, doi: [10.1016/j.icarus.2017.07.024](https://doi.org/10.1016/j.icarus.2017.07.024)
- . 2018b, *J. Geophys. Res.*, 123, 3764, doi: [10.1029/2018JA025328](https://doi.org/10.1029/2018JA025328)
- Krüger, H., Geissler, P., Horányi, M., et al. 2003, *Geophys. Res. Lett.*, 30, 210000, doi: [10.1029/2003GL017827](https://doi.org/10.1029/2003GL017827)
- Kupo, I., Mekler, Y., & Eviatar, A. 1976, *Astrophys. J., Lett.*, 205, L51, doi: [10.1086/182088](https://doi.org/10.1086/182088)
- Kurth, W. S., Hospodarsky, G. B., Kirchner, D. L., et al. 2017, *Space Science Reviews*, 213, 347, doi: [10.1007/s11214-017-0396-y](https://doi.org/10.1007/s11214-017-0396-y)
- Kurucz, R. L. 2005, *Memorie della Societa Astronomica Italiana Supplement*, 8, 14
- Marques, M. S., Zarka, P., Echer, E., et al. 2017, *Astron. Astrophys.*, 604, A17, doi: [10.1051/0004-6361/201630025](https://doi.org/10.1051/0004-6361/201630025)
- McComas, D. J., Alexander, N., Allegrini, F., et al. 2017, *Space Science Reviews*, 213, 547, doi: [10.1007/s11214-013-9990-9](https://doi.org/10.1007/s11214-013-9990-9)
- McGrath, M. A., Lellouch, E., Strobel, D. F., Feldman, P. D., & Johnson, R. E. 2004, *Satellite atmospheres*, ed. F. Bagenal, T. E. Dowling, & W. B. McKinnon (Cambridge: Cambridge University Press), 457–483
- Mendillo, M., Baumgardner, J., Flynn, B., & Hughes, W. J. 1990, *Nature*, 348, 312, doi: [10.1038/348312a0](https://doi.org/10.1038/348312a0)
- Mendillo, M., Wilson, J., Spencer, J., & Stansberry, J. 2004, *Icarus*, 170, 430, doi: [10.1016/j.icarus.2004.03.009](https://doi.org/10.1016/j.icarus.2004.03.009)
- Morabito, L. A., Synnott, S. P., Kupferman, P. N., & Collins, S. A. 1979, *Sci*, 204, 972, doi: [10.1126/science.204.4396.972](https://doi.org/10.1126/science.204.4396.972)
- Morgenthaler, D. R., & Morgenthaler, J. P. 2019, *Python aliases and shortcuts*, v1.0.1, Zenodo, doi: [10.5281/zenodo.2535735](https://doi.org/10.5281/zenodo.2535735).
<https://doi.org/10.5281/zenodo.2535735>
- Morgenthaler, J. P. 2019, *Io Input/Output facility (IoIO) control, reduction, and analysis software*, v1.0.1, Zenodo, doi: [10.5281/zenodo.2535838](https://doi.org/10.5281/zenodo.2535838).
<https://doi.org/10.5281/zenodo.2535838>
- Morgenthaler, J. P., Rathbun, J. A., Schmidt, C. A., Baumgardner, J., & Schneider, N. M. 2019, *Io Input/Output (IoIO) aperture sum data file*, v1.0, Zenodo, doi: [10.5281/zenodo.2535920](https://doi.org/10.5281/zenodo.2535920).
<https://doi.org/10.5281/zenodo.2535920>
- Nozawa, H., Misawa, H., Takahashi, S., et al. 2004, *J. Geophys. Res.*, 109, 7209, doi: [10.1029/2003JA010241](https://doi.org/10.1029/2003JA010241)
- Oliphant, T. E. 2006, *Guide to NumPy* (Provo: Trelgol Publishing)
- Radioti, A., Lystrup, M., Bonfond, B., Grodent, D., & Gérard, J.-C. 2013, *J. Geophys. Res.*, 118, 2286, doi: [10.1002/jgra.50245](https://doi.org/10.1002/jgra.50245)
- Rathbun, J. A., & Spencer, J. R. 2006, *Geophys. Res. Lett.*, 33, L17201, doi: [10.1029/2006GL026844](https://doi.org/10.1029/2006GL026844)
- Schmidt, C., Schneider, N., Leblanc, F., et al. 2018, *J. Geophys. Res.*, 123, 5610, doi: [10.1029/2018JA025296](https://doi.org/10.1029/2018JA025296)
- Schneider, N. M., & Bagenal, F. 2007, *Io's neutral clouds, plasma torus, and magnetospheric interaction* (Berlin, Heidelberg: Springer Praxis Books / Geophysical Sciences), 265–286
- Schneider, N. M., Wilson, J. K., Trauger, J. T., et al. 1991, *Sci*, 253, 1394, doi: [10.1126/science.253.5026.1394](https://doi.org/10.1126/science.253.5026.1394)
- Sinton, W. M. 1980, *Icarus*, 43, 56, doi: [10.1016/0019-1035\(80\)90087-1](https://doi.org/10.1016/0019-1035(80)90087-1)
- Steffl, A. J., Delamere, P. A., & Bagenal, F. 2006, *Icarus*, 180, 124, doi: [10.1016/j.icarus.2005.07.013](https://doi.org/10.1016/j.icarus.2005.07.013)
- . 2008, *Icarus*, 194, 153, doi: [10.1016/j.icarus.2007.09.019](https://doi.org/10.1016/j.icarus.2007.09.019)
- Tummers, B. 2006, *DataThief III*. <https://datathief.org/>
- van der Walt, S., Schönberger, J. L., Nunez-Iglesias, J., et al. 2014, *PeerJ*, 2, e453, doi: [10.7717/peerj.453](https://doi.org/10.7717/peerj.453)

- Wilson, J. K., Mendillo, M., Baumgardner, J., et al. 2002, *Icarus*, 157, 476, doi: [10.1006/icar.2002.6821](https://doi.org/10.1006/icar.2002.6821)
- Witteborn, F. E., Bregman, J. D., & Pollack, J. B. 1979, *Sci*, 203, 643, doi: [10.1126/science.203.4381.643](https://doi.org/10.1126/science.203.4381.643)
- Woodman, J. H., Cochran, W. D., & Slavsky, D. B. 1979, *Icarus*, 37, 73, doi: [10.1016/0019-1035\(79\)90116-7](https://doi.org/10.1016/0019-1035(79)90116-7)
- Yoneda, M., Kagitani, M., & Okano, S. 2009, *Icarus*, 204, 589, doi: [10.1016/j.icarus.2009.07.023](https://doi.org/10.1016/j.icarus.2009.07.023)
- Yoneda, M., Kagitani, M., Tsuchiya, F., Sakanoi, T., & Okano, S. 2015, *Icarus*, 261, 31, doi: [10.1016/j.icarus.2015.07.037](https://doi.org/10.1016/j.icarus.2015.07.037)
- Yoneda, M., Nozawa, H., Misawa, H., Kagitani, M., & Okano, S. 2010, *Geophys. Res. Lett.*, 37, 11202, doi: [10.1029/2010GL043656](https://doi.org/10.1029/2010GL043656)
- Yoneda, M., Miyata, T., Tsang, C. C. C., et al. 2014, *Icarus*, 236, 153, doi: [10.1016/j.icarus.2014.01.019](https://doi.org/10.1016/j.icarus.2014.01.019)